BBA - Molecular Cell Research 1865 (2018) 1914–1923

Contents lists available at ScienceDirect

BBA - Molecular Cell Research

journal homepage: www.elsevier.com/locate/bbamcr

Mutant p53 prevents GAPDH nuclear translocation in pancreatic cancer cells favoring glycolysis and 2-deoxyglucose sensitivity

Giovanna Butera[a], Raffaella Pacchiana[a], Nidula Mullappilly[a], Marilena Margiotta[b], Stefano Bruno[b], Paola Conti[c], Chiara Riganti[d], Massimo Donadelli[a,*]

[a] Department of Neurosciences, Biomedicine and Movement Sciences, Section of Biochemistry, University of Verona, Verona, Italy
[b] Food and Dug Department, University of Parma, Parma, Italy
[c] Department of Pharmaceutical Sciences, University of Milan, Milano, Italy
[d] Department of Oncology, University of Torino, Torino, Italy

ARTICLE INFO

Keywords:
Mutant p53
Pancreas cancer
GAPDH
AMPK
AKT
SIRT1

ABSTRACT

Pancreatic ductal adenocarcinoma (PDAC) is one of the most aggressive and devastating human malignancies. In about 70% of PDACs the tumor suppressor gene *TP53* is mutated generally resulting in conformational changes of mutant p53 (mutp53) proteins, which acquire oncogenic functions triggering aggressiveness of cancers and alteration of energetic metabolism. Here, we demonstrate that mutant p53 prevents the nuclear translocation of the glycolytic enzyme glyceraldehyde-3-phosphate dehydrogenase (GAPDH) stabilizing its cytoplasmic localization, thus supporting glycolysis of cancer cells and inhibiting cell death mechanisms mediated by nuclear GAPDH. We further show that the prevention of nuclear localization of GAPDH is mediated by both stimulation of AKT and repression of AMPK signaling, and is associated with the formation of the SIRT1:GAPDH complex. By using siRNA-GAPDH or an inhibitor of the enzyme, we functionally demonstrate that the maintenance of GAPDH in the cytosol has a critical impact on the anti-apoptotic and anti-autophagic effects driven by mutp53. Furthermore, the blockage of its mutp53-dependent cytoplasmic stabilization is able to restore the sensitivity of PDAC cells to the treatment with gemcitabine. Finally, our data suggest that mutp53-dependent enhanced glycolysis permits cancer cells to acquire sensitivity to anti-glycolytic drugs, such as 2-deoxyglucose, suggesting a potential personalized therapeutic approach in human cancers carrying mutant *TP53* gene.

1. Introduction

Pancreatic cancer is one of the most frequent causes of tumor-associated deaths, and its incidence has recently increased in the western world [1]. Pancreatic ductal adenocarcinoma (PDAC) is the most common type of pancreatic malignancy and has a poor prognosis, with a dismal overall 5-year survival rate of 5% [2]. The standard chemotherapy regimen is still based on gemcitabine [3] since the ever-growing understanding of the complex genetic, epigenetic and metabolic alterations as well as of the equally complex interplay of cancer cells with stromal cells, immune cells and endothelial cells has not yet resulted in a dramatic change in the overall outcome for PDAC patients [4].

One of the most frequent alterations revealed in PDAC patients (~70%) is the missense mutations of the *TP53* tumor suppressor gene generating mutant p53 isoforms (mutp53s), which can acquire new biological properties referred as gain-of-function (GOF) [5]. In addition to the loss of the tumor suppression function of wild-type p53 (WTp53), GOF mutp53 proteins contribute to the maintenance and stimulation of cancer cell growth through the acquisition of oncogenic functions [5,6]. Such GOF activities dramatically alter tumor cell characteristics, primarily through their interactions with other cellular proteins and regulation of cancer cell transcriptional programs [7]. Several studies have elucidated that mutp53s are able to modulate the expression of a set of genes through direct interaction with a number of transcription factors, such as NF-Y, E2F1, E2F4, NF-κB p65, NF-κB p50, SREBP1 and vitamin D receptor, thus regulating a panel of biological processes ranging from metabolic reprogramming to the inhibition of apoptosis addressed to triggering of cancer progression [6,8–11]. In particular, mutp53 was reported to promote glycolysis and glucose metabolism to stimulate cancer cell growth [12,13], in contrast to the glycolytic inhibitory role of the tumor suppressor WTp53. However, the precise molecular

* Corresponding author at: Department of Neurosciences, Biomedicine and Movement Sciences, Section of Biochemistry, University of Verona, Strada Le Grazie 8, 37134 Verona, Italy.
E-mail address: massimo.donadelli@univr.it (M. Donadelli).

https://doi.org/10.1016/j.bbamcr.2018.10.005
Received 12 June 2018; Received in revised form 14 September 2018; Accepted 2 October 2018
Available online 05 October 2018

mechanisms involved in this aberrant regulation of metabolism by mutp53 isoforms are still incomplete.

Intriguingly, in addition to their canonical roles in glycolysis, recent studies gradually uncovered some non-metabolic functions of glycolytic enzymes in tumorigenesis and regulation of cancer cell fate [14]. Specifically, beyond glycolysis several reports have demonstrated that the enzyme glyceraldehyde-3-phosphate dehydrogenase (GAPDH) has a variety of other functions, including DNA repair, transcriptional regulation, membrane fusion and transport, autophagy, and cell death [15–17]. The pleiotropic roles of GAPDH are strictly associated to its intracellular localization, which is not restricted to the cytosol for glycolytic energy production. Indeed, GAPDH is detected in other subcellular compartments, such as nuclei in which it exerts a critical role in the regulation of cell death-related gene transcription, stimulation of apoptosis and modulation of cell fate. Post-translational modifications of the enzyme, including phosphorylation, oxidation, acetylation, glycosylation, poly ADP-ribosylation, and pyruvylation [18–20], and/or its binding with other molecules [21] are mechanisms described to be involved in the GAPDH nuclear translocation with consequent induction of anti-proliferative effects. For these reasons GAPDH has received considerable attention as an appealing drug target for cancer therapy [22].

In the present study, we demonstrate that GOF mutp53 stabilizes the cytosolic localization of GAPDH avoiding its nuclear transport. This contributes to support glycolysis and lactate secretion conferring enhanced sensitivity of cancer cells to metabolic drugs, as the glycolytic inhibitor 2-deoxyglucose. We further demonstrate that the mechanisms promoted by mutp53 to prevent the nuclear translocation of GAPDH and its nuclear cell death-related effects include AMPK inhibition and AKT stimulation, as well as the enhanced interaction between GAPDH and SIRT1.

2. Material and methods

2.1. Cell culture

Pancreatic adenocarcinoma PaCa3, Panc1 and AsPC1 cell lines were grown in RPMI 1640 medium (Thermo Fisher, Milan, Italy), supplemented with 10% FBS and 50 μg/ml gentamicin sulfate (BioWhittaker, Lonza, Bergamo, Italy), and incubated at 37 °C with 5% CO_2. These cell lines were kindly provided by Dr. Aldo Scarpa (University of Verona, Italy) and previously characterized for their genetic profile [23]. The clones C9 (mock) and H1 (stably expressing mutant p53-R273H) of the p53-null H1299 cells were kindly provided by Dr. Riccardo Spizzo (Centro di Riferimento Oncologico, National Cancer Institute, Aviano, Italy). All the cell lines were routinely tested to confirm lack of *Mycoplasma* spp. infection.

2.2. Drugs and chemicals

Gemcitabine (2′,2′-difluoro-2′-deoxycytidine; GEM) was provided by Accord Healthcare (Milan, Italy) and solubilized in sterile bi-distilled water. 2-deoxyglucose (2-DG) was obtained from Sigma (Milan, Italy), solubilized bi-distillated sterile water and stored at −80 °C until use. The GAPDH inhibitor (*S*)-benzyl-2-amino-2-(*S*)-3-bromo-4,5-dihydroisoxazol-5-yl-acetate (AXP3009) has been designed and synthetized in the laboratory of Dr. Paola Conti at the Department of Pharmaceutical Sciences (University of Milan, Italy). AXP3009 was solubilized in methanol and stored at −80 °C. Bruno et al. previously reported the chemical structure and the synthesis of AXP3009 compound [24]. The AKT inhibitor (SH-5) and the AMPK activator (AICAr) were obtained from Sigma, solubilized in DMSO and bi-distillated sterile water, respectively, and stored at −20 °C until use.

2.3. Liposome-mediated transient cell transfection

Exponentially growing cells were seeded in 96-well plates or in 60 mm cell culture plates. The ectopic expression of mutant p53 isoforms in AsPC1 p53-null cells was carried out transfecting pcDNA3-mutp53R273H or pcDNA3-mutp53R175H expression vectors, or their relative mock vector (pcDNA3). Wild-type and mutant p53 protein expression was transiently knocked-down by transfection with pRSUPER-p53 vector or its negative control (pRSUPER), kindly provided by Dr. Agami (The Netherlands Cancer Institute, Amsterdam). The silencing transfections were carried out for 48 h using Lipofectamine 3000 (Thermo Fisher), according to the manufacturer's instructions. Knock-down of GAPDH expression was obtained by transfecting cells with specific GAPDH small interfering siRNA or with a siRNA-CTRL (negative control) purchased from Life Technologies. Cells were transfected by siRNA at a final concentration of 50 nM using Lipofectamine 3000.

2.4. Lentiviral cell transduction

To silence R273H mutp53 expression in Panc1 cells, we used plasmid pLKO.1 puro-vector encoding *TP53*-shRNA (TRCN0000003756 Sigma-Aldrich) indicated as p53-SH1. As negative control we used a non-target shRNA control (SHC016; Sigma-Aldrich) indicated as p53-NT. To generate viral particles, 293FT cells (Thermo Fisher) were transfected using pLKO.1 shRNA DNA vector together with ViraPower Lentiviral Packaging Mix (pLP1, pLP2 and pLP/VSV-G) (Thermo Fisher). Seventy-two hours later, viral supernatant was collected and transducing units per ml of supernatant were determined by limiting dilution titration in cells. A MOI (multiplicity of infection) of 5 to 1 (5 transducing viral particles to 1 cell) was used for transducing cells using Polybrene (Sigma-Aldrich) at a final concentration of 8 μg/ml to increase transduction efficiency. Twenty-four hours after transduction, puromycin selection (2 μg/ml) was performed for 48 h and mutant *TP53*-silenced cells were used for experiments.

2.5. Cell proliferation assay

Cells were seeded in 96-well plates (5×10^3 cells/well) and the day after transfected with the indicated constructs (see figure legends) and incubated with various compounds at the indicated conditions. At the end of the treatments, cell growth was measured by Crystal Violet assay (Sigma) according to the manufacturer's protocol, and absorbance was measured by spectrophotometric analysis (A_{595nm}).

2.6. Soft agar colony formation assay

Anchorage-independent growth was performed in soft agar. Briefly, 5×10^4 H1299 cells, mock and R273H clones, were resuspended in complete DMEM medium containing 0.6% agarose low-gelling temperature (A9045 - Sigma Aldrich, Milan, Italy) and seeded into 6-well plates containing 1.5 ml layer of solidified 1% agarose low-gelling temperature. After seeding the cells were untreated or treated with 50 μM AXP3009. Culture medium (100 μl each well) was added twice weekly. After 21 days, cells were fixed using a solution of 4% Crystal Violet containing 1% ethanol. At the end of the growth period, colonies were photographed with 10× objective under an automated microscope (EVOS FL Auto, Thermo Fisher Scientific, Waltham, MA, USA Italy).

2.7. Apoptosis assay

Cells were seeded in 96-well plates (5×10^3 cells/well) and, the day after, were transfected with the indicated constructs (see figure legends) and incubated with various compounds at the indicated conditions. At the end of the treatments, cells were fixed with 2%

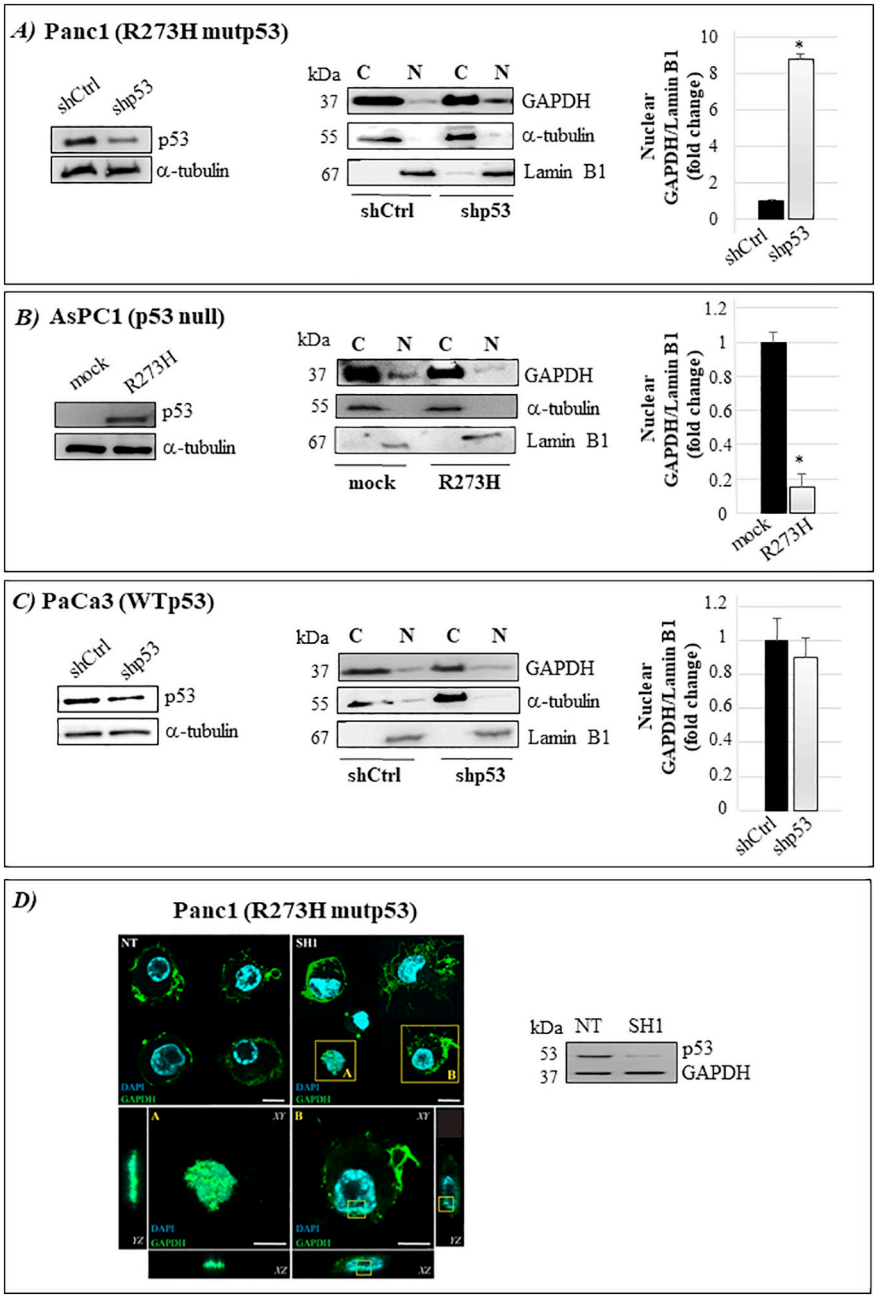

Fig. 1. Mutant p53 prevents GAPDH nuclear translocation. *A–C*) Cytosolic and nuclear extracts were used for Western blotting of GAPDH, α-tubulin and Lamin B1 in Panc1 and PaCa3 cell lines transfected with pRSuper-p53 or mock vector, or in AsPC1 cells transfected with plasmids for R273H mutant p53 expression or its negative control. α-tubulin and Lamin B1 have been used as controls of the quality of the cytoplasmic and nuclear protein fractions, respectively. The amount of nuclear GAPDH in each extract was quantified using NIH Image J software and normalized to the amount of Lamin B1. Statistical analysis *p < 0.05 Shp53 vs ShCtrl in Panc1 cells and *p < 0.05 R273H vs mock in AsPC1 cells. *D*) Transduced Panc1 cells with vector encoding *TP53*-shRNA indicated as SH1 or its non-target shRNA control indicated as non-target (NT). In NT image, the GAPDH (green signal) is mainly localized into the cytoplasm and on the cell membrane. 48 h after transduction, the enzyme is visible also into the nuclei (blue signal). *Inset A*: the cell is shown with a higher magnification. This cell is presumably undergoing apoptosis and the enzyme is clearly visible inside the nucleus (as shown by the orthogonal projection, XZ and YZ). *Inset B*: in the shown cell, the GAPDH (green spots) begins to localize in the nucleus as it can be appreciated from the orthogonal projection XZ and YZ (yellow squares). Scale bar: 10 μm. (For interpretation of the references to color in this figure legend, the reader is referred to the web version of this article.)

paraformaldehyde in PBS at RT for 30 min, then washed twice with PBS and stained with annexinV/FITC (Bender MedSystem, Milan, Italy) in binding buffer (10 mM HEPES/NaOH pH 7.4, 140 mM NaCl and 2.5 mM $CaCl_2$) for 10 min at RT in the dark. Finally, cells were washed with binding buffer solution and fluorescence was measured by using a multimode plate reader (Ex_{485nm} and Em_{535nm}) (GENios Pro, Tecan, Milan, Italy). The values were normalized on cell proliferation by Crystal Violet assay.

2.8. Monodansylcadaverine staining and autophagosome formation assay

To quantify the induction of autophagy, cells were incubated with the fluorescent probe monodansylcadaverine (MDC) (Sigma), accordingly with the guidelines for studying autophagy [25]. MDC is a selective marker for acidic vesicular organelles, such as autophagic vacuoles. Briefly, cells were seeded in 96-well plates (5×10^3 cells/well) and treated with various compounds as indicated in the figure legend. At the end of the treatments, cells were incubated in culture medium containing 50 μM MDC at 37 °C for 15 min. Cells were then washed with Hanks buffer (20 mM Hepes pH 7.2, 10 mM glucose, 118 mM NaCl, 4.6 mM KCl, and 1 mM $CaCl_2$) and fluorescence was measured using a multimode plate reader (Ex_{340nm} and Em_{535nm}) (GENios Pro, Tecan). The values were normalized on cell proliferation by Crystal Violet assay.

2.9. RNA isolation and quantitative real-time PCR analysis

Total RNA was extracted from 10^6 cells using TRIzol Reagent (Thermo Fisher) and 1 μg of RNA was reverse transcribed using first-strand cDNA synthesis. Real-time quantification was performed in triplicate samples by SYBR Green detection chemistry with Power SYBR Green PCR Master Mix (Applied Biosystems, Carlsbad, CA, USA) on a 7900 HT Fast Real-Time PCR System (Thermo Fisher). Normalization was performed analyzing the ribosomal protein large P0 (RPLP0) mRNA expression level. The primers used were: GAPDH For, 5′-ATCA

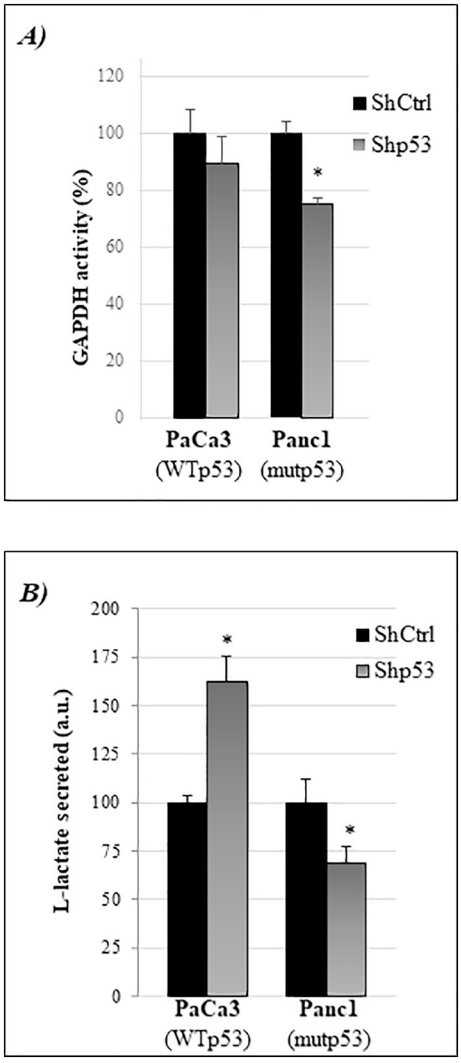

Fig. 2. Mutant p53 enhances GAPDH glycolytic activity and L-lactate secretion. *A*) GAPDH activity was quantified in Panc1 and PaCa3 cells transfected with pRSuper-p53 vector or its negative control for 48 h. Statistical analysis *p < 0.05 Shp53 vs ShCtrl. *B*) Panc1 and PaCa3 cells were transfected with pRSuper-p53 vector or its negative control for 48 h. L-Lactic acid level in the culture medium has been analyzed by measuring the absorbance at 340 nm and the L-lactic acid concentration has been calculated as detailed in Material and methods. Statistical analysis *p < 0.05 Shp53 vs ShCtrl.

GCAATGCCTCCTGCAC-3′; GAPDH Rev., 5′-TGGTCATGAGTCCTTCC ACG-3′; RPLP0 For, 5′-ACATGTTGCTGGCCAATAAGGT-3′ and RPLP0 Rev., 5′-CCTAAAGCCTGGAAAAAGGAGG-3′. The thermal cycle reaction was performed as follows: 95 °C for 10 min followed by 40 cycles at 95 °C for 15 s and 60 °C for 1 min. The average of cycle threshold of each triplicate was analyzed according to the $2^{(-\Delta\Delta Ct)}$ method. Three independent experiments were performed for each assay condition.

2.10. Subcellular fractionation and immunoblot analysis

Cells were washed with PBS and scraped into hypotonic buffer (10 mM HEPES pH 8.0, 10 mM KCl, 0.1% Igepal CA-630, 1.5 mM $MgCl_2$, 1 mM NaF, 0.5 mM Na_3VO_4, 0.5 mM DTT, 1 mM PMSF and 1 × protease inhibitor cocktail). The suspension was incubated on ice for 10 min and after centrifugation at 300 ×*g* for 10 min at 4 °C, the supernatant was used as the cytoplasmic fraction. The pellet was washed twice with PBS and reconstituted in RIPA buffer (100 mM Tris HCl pH 8.0, 1% Triton X-100,100 mM NaCl, 0.5 mM EDTA and 1 × protease inhibitor cocktail). The suspension was incubated on ice for 15 min. After centrifugation at 15,000 ×*g* for 10 min, the resultant supernatant was used as the nuclear fraction. To obtain whole cell lysates, cells were harvested, washed in PBS, and re-suspended in lysis buffer in the presence of phosphatase and protease inhibitors (50 mM Tris–HCl pH 8.0, 150 mM NaCl, 1% Igepal CA-630, 0.5% Na-Doc, 0.1% SDS, 1 mM Na_3VO_4, 1 mM NaF, 2.5 mM EDTA, 1 mM PMSF, and 1 × protease inhibitor cocktail). After incubation on ice for 30 min, the lysates were centrifuged at 5000 ×*g* for 10 min at 4 °C and the supernatant fractions were used for Western blot analysis.

Protein extracts (50 μg/lane for whole cell lysate immunoblots and 5 μg/lane for cytoplasmic and nuclear cell lysate immunoblots) were resolved on a 12% SDS-polyacrylamide gel and electro-blotted onto PVDF membranes (Millipore, Milan, Italy). Membranes were blocked in 5% low-fat milk in TBST (50 mM Tris pH 7.5, 0.9% NaCl, 0.1% Tween 20) for 1 h at room temperature (RT) and probed overnight at 4 °C with anti-phospho(Ser473)-AKT (1:2000; Cell Signaling Technology, Danvers, MA, USA, #4060), anti-AKT (1:1000; Cell Signaling #9272), anti-α-tubulin (1:2500; Oncogene, La Jolla, CA, USA, #CP06-100UG), anti-phospho(Thr172)AMPKα (1:1000) (Cell Signaling, #2535), anti-AMPKα (1:1000) (Cell Signaling, #2603), anti-glyceraldehyde 3-phosphate dehydrogenase GAPDH (G-9) (1:1000; Santa Cruz #sc-365062), anti-LaminB1 (A-11) (1:1000; Santa Cruz #sc-377000), anti-p53 (BP 53.12) (1:2000; Santa Cruz #sc-81168), anti-Sirt1(D739) (1:1000, Cell Signaling #2493). The immunocomplexes were visualized by chemiluminescent substrates (Amersham Pharmacia Biotech, Milan, Italy) using ChemidocMP imaging system (Bio-Rad Laboratories, Milan, Italy) and the intensity of the chemiluminescence signal was quantified using NIH Image J software (http://rsb.info.nih.gov/nih-image/).

2.11. Immunofluorescence imaging of GAPDH subcellular localization

After lentiviral transduction, Panc1 cells were fixed in 4% paraformaldehyde for 15 min and, after 4 changes (10 min each) of PBS, were permeabilized with 0.1% Triton X–100 for 5 min in PBS. To saturate unspecific binding sites, the cells were incubated for 45 min at RT with a blocking solution containing 5% BSA and 0.05% Triton X-100 in PBS. Samples were then incubated overnight at 4 °C with anti-GAPDH (1:250; Santa Cruz #sc-365062) primary antibody diluted in blocking solution. After 3 washes with PBS (10 min each), cells were incubated for 1 h at RT in the dark with specific secondary antibodies (1 μg/ml) conjugated with Alexa Fluor-488 (Molecular Probes, Eugene, OR, USA). The incubation with secondary antibody was followed by 10 min incubation at RT with 1 μg/ml of 4′,6-diamidino-2-phenylindole dihydrochloride (DAPI, Sigma-Aldrich). Samples were mounted in anti-bleaching medium (Dako Fluorescent Mounting Medium). The negative control procedure omitted the primary antibody. Pictures were acquired under a Leica TCS SP5 AOBS laser confocal microscope (Leica-Microsystems, Wezlar, Germany). A 40×/1.25 NA oil-immersion objective (HCX PL APO 40 × 1.25 OIL UV, Leica-Microsystem) was used.

2.12. Immunoprecipitation assay

Cell extracts were solubilized in lysis buffer with 150 mM Hepes pH 7.5, 300 mM NaCl, 1% Triton-×100, phosphatase and protease inhibitors. Cells were harvested and lysed in lysis buffer and cleared by centrifugation. For each immunoprecipitation, 1 μg of antibody and 1 μg of rabbit or sheep IgG (Santa Cruz Biotech) as control were used. To immunoprecipitate we used an anti-GAPDH antibody from Santa Cruz (sc-365062). 1 mg of pre-cleared protein extracts were diluted in lysis buffer containing 0.05% BSA and incubated with Dynabeads® Protein G (Thermo Fisher) and antibodies, according to the manufacturer's instructions. Bead-bound immunocomplexes were rinsed with lysis buffer and eluted in 50 μl of SDS sample buffer for Western blotting. Immunoblotting was performed using the following primary antibodies: anti-Sirt1 (D739) (1:1000, Cell Signaling #2493), anti-GAPDH

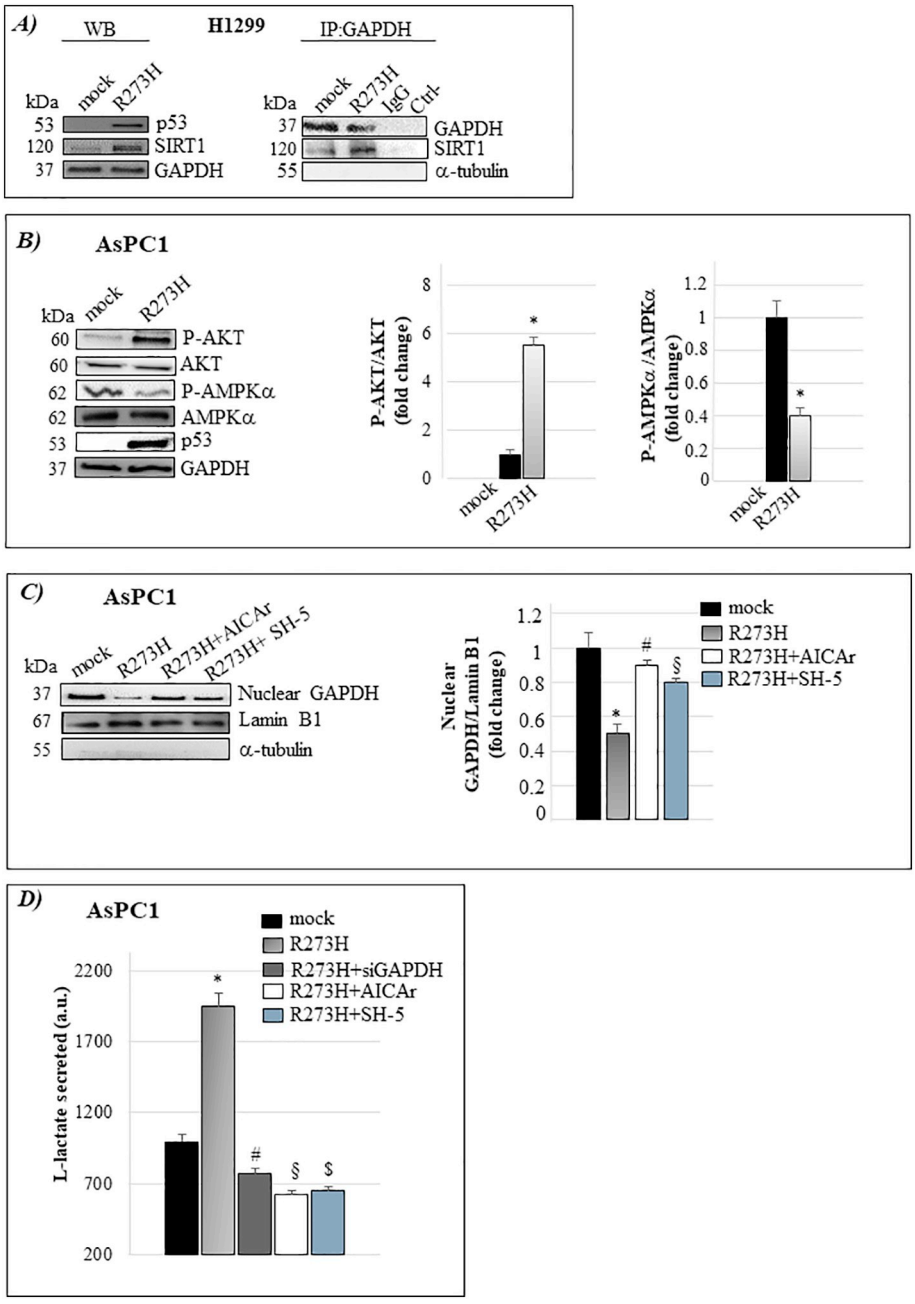

Fig. 3. Prevention of nuclear localization of GAPDH by mutp53 is mediated by regulation of SIRT1:GAPDH complex and of AMPK and AKT pathways. *A*) Cell lysates from p53-null H1299 cancer cells (C9 clone) and H1299 stably expressing R273H mutp53 (H1 clone) were used to perform Western blotting by loading 30 µg of protein extracts and probed with the indicated antibodies. *Left panel*: GAPDH was used as control of equal protein loading. *Right panel*: GAPDH was immunoprecipitated from protein extracts of H1299 cell C9 clone (mock) or H1 clone stably expressing R273H mutp53 using anti-mouse GAPDH antibody (IP: GAPDH) and Western blotting was performed using anti-SIRT1 antibody. Negative control ($Ctrl^-$) corresponds to lysis buffer without protein extracts immunoprecipitated with anti-GAPDH as described for mock or R273H samples. Protein extracts from H1299 cells (C9 mock clone) were also immunoprecipitated with an equal amount of mouse IgG as control. The blot exhibits equivalent GAPDH levels and the absence of α-tubulin expression in C9 and H1 clone samples as control of the quality of the immunoprecipitation. *B*) Western blotting was performed using 40 µg of whole cell protein extracts from AsPC1 transfected with plasmids for R273H mutant p53 expression or its negative control (mock) and probed with the indicated antibodies. For quantitative analysis, bands were quantified using NIH Image J software and normalized to the amount of GAPDH. Statistical analysis * $p < 0.05$ R273H vs mock. *C*) AsPC1 cells were transfected with the vectors for the ectopic expression of p53-R273H or its mock control for 48 h and treated with 2 mM AICAr for 72 h or 15 µM SH-5 for 48 h. Western Blot analysis was performed using whole cell extracts of AsPC1 and probed with the indicated antibodies. α-tubulin and Lamin B1 have been used as controls of the quality of the nuclear protein fraction. Statistical analysis *$p < 0.05$ R273H vs mock; $^{\#}p < 0.05$ R273H + AICAr vs R273H; $^{\S}p < 0.05$ R273H + SH-5 vs R273H. *D*) AsPC1 cells were transfected with the vectors for the ectopic expression of p53-R273H or its mock control for 48 h and for the knock-down of GAPDH using 50 nM siRNA-GAPDH for 48 h. AsPC1 cells were treated 2 mM AICAr for 72 h or 15 µM SH-5 for 48 h. L-Lactic acid level in the culture medium has been analyzed as detailed in Material and methods. Statistical analysis *$p < 0.05$ R273H vs mock; $^{\#}p < 0.05$ R273H + siGAPDH vs R273H; $^{\S}p < 0.05$ R273H + AICAr vs R273H; $^{\$}p < 0.05$ R273H + SH-5 vs R273H.

(G-9) (1:1000; Santa Cruz #sc-365062), anti-α-tubulin (1:2500; Oncogene #CP06-100UG).

2.13. L-Lactic acid quantification assay

AsPC1 cells were seeded in 96-well plates (5×10^3 cells/well) and transfected for 48 h. At the end of the treatments, culture medium has been harvested, centrifuged at 1500 × *g* for 10 min and diluted six-fold in H_2O. For each sample, 25 µl has been analyzed in a final reaction volume of 500 µl (Megazyme, #K-LATE 07/14). Absorbance at 340 nm has been read after 10 min. The activation of the reaction and L-lactic acid concentration (g/l) has been calculated according to the manufacturer's instructions. The amount of L-lactic acid secreted by the cells in each sample was calculated by subtracting the amount of L-lactic acid in the medium (without cells) from the amount of L-lactic acid in the medium from each sample. The values obtained were normalized to the number of cells in each well.

2.14. GAPDH activity

Cells were resuspended in 0.2 ml of an ice-cold buffered solution containing 200 mM NaCl, 1 mM EDTA, 20 mM CHAPS and 10% sucrose at pH = 7 and disrupted with three freeze-thaw cycles. The total soluble protein content of the cell lysates was assessed by measuring the absorbance at 280 nm using a Cary4000 spectrophotometer (Agilent Technologies). Aliquots of 10 µl were assayed for GAPDH activity using a modified version of the Ferdinand assay [26] in a buffered solution containing 10 mM triethanolamine, 10 mM sodium arseniate, 5 mM EDTA, 1.5 mM NAD^+ and 2.2 mM DL-glyceraldehyde 3-phosphate. NADH formation at 25 °C was monitored at 340 nm. Each assay was carried out at least in duplicate. The initial velocity was determined by linear fitting of the initial phase of the kinetics. The ratio between GAPDH activity and total soluble protein content was calculated for each cell lysate.

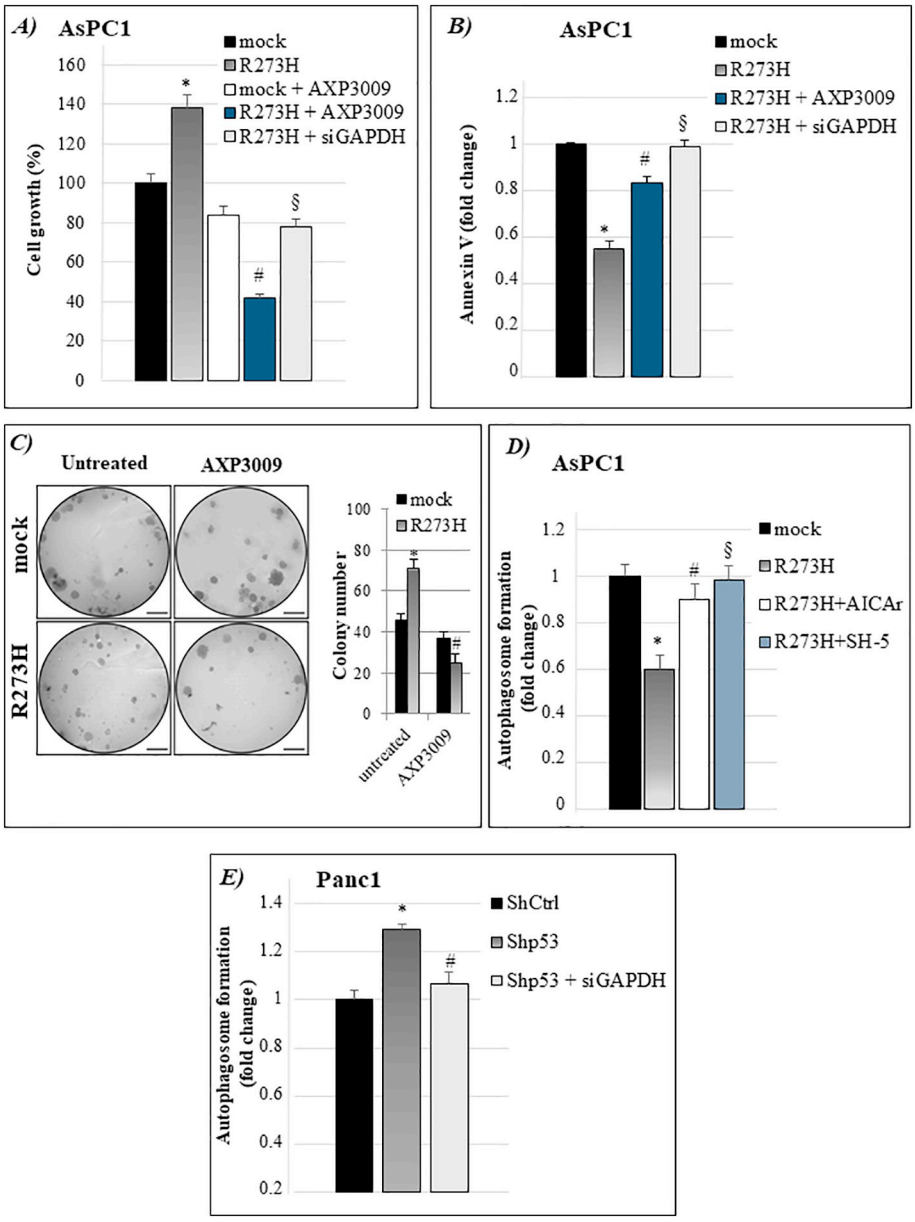

Fig. 4. GAPDH cytosolic stabilization contributes to the oncogenic effects of mutp53. *A*) Cell proliferation was measured by Cristal Violet assay and *B*) apoptosis was determined by the annexinV binding assay. AsPC1 cells were transfected with plasmids for R273H mutant p53 over-expression or its mock vector and for the knock-down of GAPDH using 50 nM siRNA-GAPDH for 48 h. The cells were also treated with 100 μM AXP3009 compound for 48 h. Statistical analysis *$p < 0.05$ R273H vs mock; $^{\#}p < 0.05$ R273H + AXP3009 vs R273H; $^{\S}p < 0.05$ R273H + siGAPDH vs R273H. *C*) Representative images of soft agar colony assay. Upon 21 days of H1299 cell culture, the number of colonies in mock cells and mutp53 R273H cells, untreated or treated with 50 μM AXP3009, was quantified by ImageJ software after staining with Crystal Violet. Results were shown as mean ± SEM of three independent experiment (right panel). Scale bar: 200 μm. Statistical analysis *$p < 0.05$ R273H vs mock; $^{\#}p < 0.05$ R273H + AXP3009 vs R273H. *D*) Autophagosome formation assay through the incorporation of the MDC probe in AsPC1 cells transfected and treated with 2 mM AICA-R for 72 h or 15 μM SH-5 for 48 h. Statistical analysis *$p < 0.05$ R273H vs mock; $^{\#}p < 0.05$ R273H + AICAr vs R273H; $^{\S}p < 0.05$ R273H + SH-5 vs R273H. *E*) Autophagosome formation assay in Panc1 cells transfected with pRSuper-p53 vector (Shp53) or its negative control (ShCtrl), in the absence or presence of siRNA-GAPDH for 48 h. Statistical analysis *$p < 0.05$ shp53 vs shCtrl; $^{\#}p < 0.05$ shp53 + siGAPDH vs shp53.

2.15. Statistical analysis

ANOVA analysis with GraphPad Prism 5 software or two-tailed *t*-test were used to calculate p values. Statistically significant results were referred with a p-value < 0.05. Values are the means of three independent experiments (± SD).

3. Results

3.1. Mutant p53 prevents GAPDH nuclear translocation

To study the functional role of mutp53 proteins in the regulation of the intracellular distribution of GAPDH, we modulated p53 expression in PDAC Panc1 and PaCa3 cell lines having mutant or WT *TP53* gene, respectively, by using liposome-mediated transient transfection assay and we analyzed the abundance of GAPDH in the cytosolic and nuclear fractions of the cells. When Panc1 cells were knocked-down for mutp53 expression (left panel), the GAPDH expression level in the nuclear fraction increased revealing a role for mutp53 in the prevention of the nuclear translocation of the enzyme (Fig. 1A). Consistent with this, the exogenous expression of R273H mutp53 in AsPC1 cells (null for p53 expression) (left panel) produced a drastic decrease of the GAPDH expression in nuclei (Fig. 1B). To investigate whether this is a phenomenon specifically acquired by mutant proteins we knocked-down WTp53 (left panel) and analyzed cytosolic and nuclear GAPDH distribution, revealing that the WTp53 counterpart was not able to regulate the enzymatic nuclear translocation (Fig. 1C). To check the purity of cytosolic and nuclear subcellular fractions we tested the abundance of α-tubulin and of Lamin B1, which are specifically expressed in cytosol and nucleus of the cells, respectively (Fig. 1A–C). We further strengthened these data through lentivirus-mediated transduction and immunofluorescence analysis by confocal microscopy using a different sequence to knock-down mutant p53 expression (p53-SH1) or its negative non-targeted control (p53-NT) in PDAC Panc1 cells. Fig. 1D shows that mutp53 silencing unchanged the expression level of GAPDH (right panel), but it prompted GAPDH nuclear positivity as revealed also by XY, XZ and YZ orthogonal projections of confocal images.

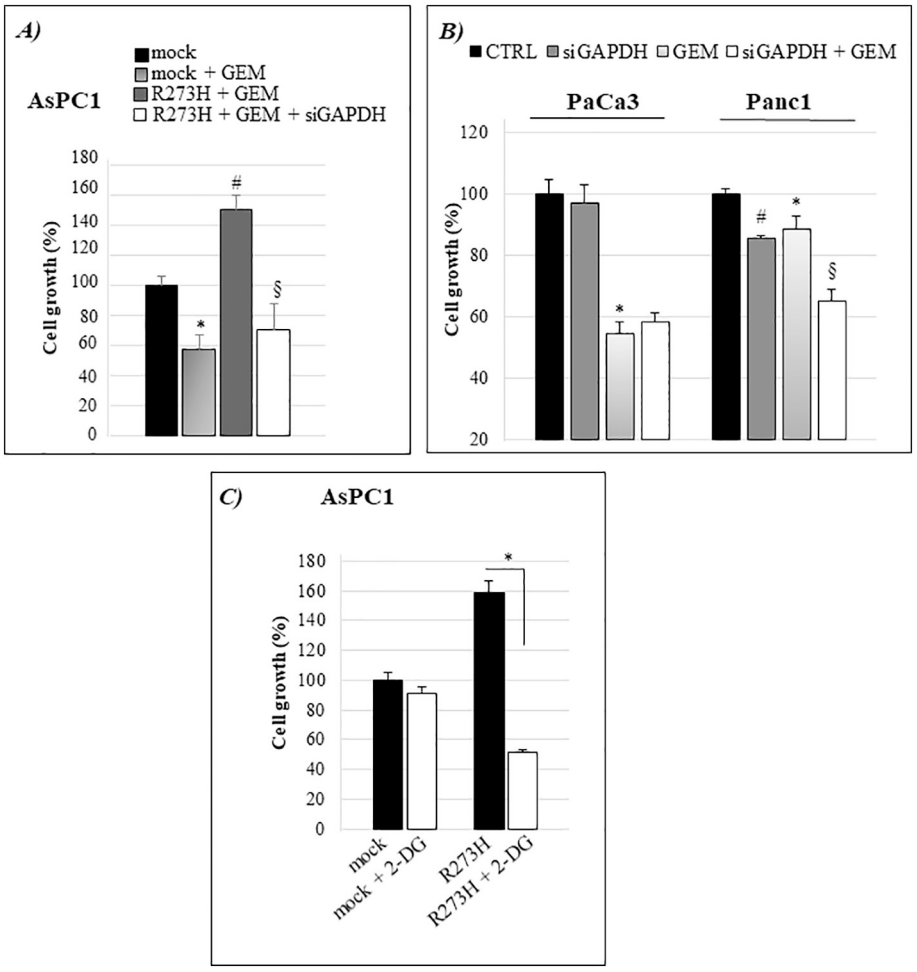

Fig. 5. GAPDH cytosolic stabilization confers chemoresistance to gemcitabine and sensitizes cells to 2-deoxyglucose. *A*) Cell proliferation was measured by Cristal Violet assay in AsPC1 transfected cells and treated with 1 μM gemcitabine (GEM) for 48 h. Statistical analysis *$p < 0.05$ mock + GEM vs mock; #$p < 0.05$ R273H + GEM vs mock + GEM; §$p < 0.05$ R273H + GEM + siGAPDH vs R273H + GEM. *B*) Cell proliferation was measured by Cristal Violet assay in WTp53 PaCa3 cells and mutp53 Panc1 cells transfected with siRNA GAPDH and/or treated with 1 μM gemcitabine (GEM) for 48 h. #$p < 0.05$ siGAPDH vs CTRL; *$p < 0.05$ GEM vs CTRL; §$p < 0.05$ siGAPDH + GEM vs GEM. *C*) Cell proliferation was measured by Cristal Violet assay in AsPC1 cells transfected as indicated and treated with 5 mM 2-DG for 48 h. Statistical analysis *$p < 0.05$ R273H + 2-DG vs R273H.

3.2. Mutant p53 enhances GAPDH glycolytic activity and L-lactate secretion

We further explored whether the stabilization of cytosolic GAPDH by mutp53 resulted in an enhanced glycolytic activity of the enzyme. Consistent with results reported in Fig. 1, Fig. 2A shows that mutp53 knock-down in Panc1 cells decreased GAPDH activity, which remained unchanged after WTp53 silencing in PaCa3 cells. Overall, in our experimental model we observed that WTp53 and mutp53 have dual opposite effects on the secretion of L-lactate, the metabolic compound generated by the glycolytic pathway. Fig. 2B shows that L-lactate secretion was enhanced by mutp53, consistent with the cytosolic stabilization of GAPDH, while the WTp53 counterpart produced an inhibitory effect on L-lactate secretion, consistent with its overall negative effects on glycolysis [27].

3.3. Prevention of nuclear localization of GAPDH by mutp53 is mediated by regulation of SIRT1:GAPDH complex and of AMPK and AKT pathways

Since it has been described that the binding of SIRT1 to GAPDH retains the latter protein in the cytosol as a mechanism to protect cytosolic GAPDH from nuclear translocation [21], we investigated whether mutp53 might stimulate SIRT1:GAPDH interaction. The large amount of protein extract used for the immunoprecipitation assay was obtained by a clone of H1299 cancer cells stably expressing R273H mutp53, which we already used to study the oncogenic effects of mutp53s [28]. Fig. 3A shows that H1299 cancer cells stably expressing R273H mutp53 presented enhanced levels of SIRT1 as compared to a mock clone of the same cells (left panel). Furthermore, immunoprecipitation assay revealed that SIRT1:GAPDH interaction was increased in R273H mutp53 expressing cells, as compared to mock (right panel), suggesting an involvement for this complex in the prevention of nuclear localization of GAPDH driven by mutp53 in cancer cells.

Moreover, since GAPDH cellular distribution can also be regulated by post-translational modifications of the enzyme, we tested whether mutp53 can modulate AMPK and AKT signaling pathways, which are described to be involved in GAPDH phosphorylation in different amino acidic residues of the enzyme resulting in the inhibition or in the stimulation of GAPDH nuclear translocation, respectively [29,30]. Fig. 3B shows that mutp53 overexpression in p53-null PDAC AsPC1 cells strongly stimulated AKT signaling (P-AKT/AKT ratio) and inhibited AMPK signaling (P-AMPK/AMPK ratio). To investigate the role of AMPK and AKT regulation on the prevention of nuclear localization of GAPDH by mutp53 we treated cells with the AMPK activator AICAr or with the AKT inhibitor SH-5. Fig. 3C reports that the decrease of nuclear GAPDH by mutp53 was recovered by AICAr or SH-5 treatment. Accordingly, the increased level of secreted L-lactate by mutp53 was reversed after GAPDH silencing or cell treatment with AICAr or SH-5 (Fig. 3D). Altogether these results demonstrated that mutp53 adopted different mechanisms to prevent GAPDH nuclear translocation sustaining cytosolic glycolysis, as the interaction of the glycolytic enzyme with SIRT1 as well as the inhibition of AMPK and stimulation of AKT pathways.

3.4. GAPDH cytosolic stabilization contributes to the oncogenic effects of mutp53

To investigate the functional role of GAPDH cytosolic stabilization on the oncogenic effects of mutp53 we tested PDAC cell proliferation

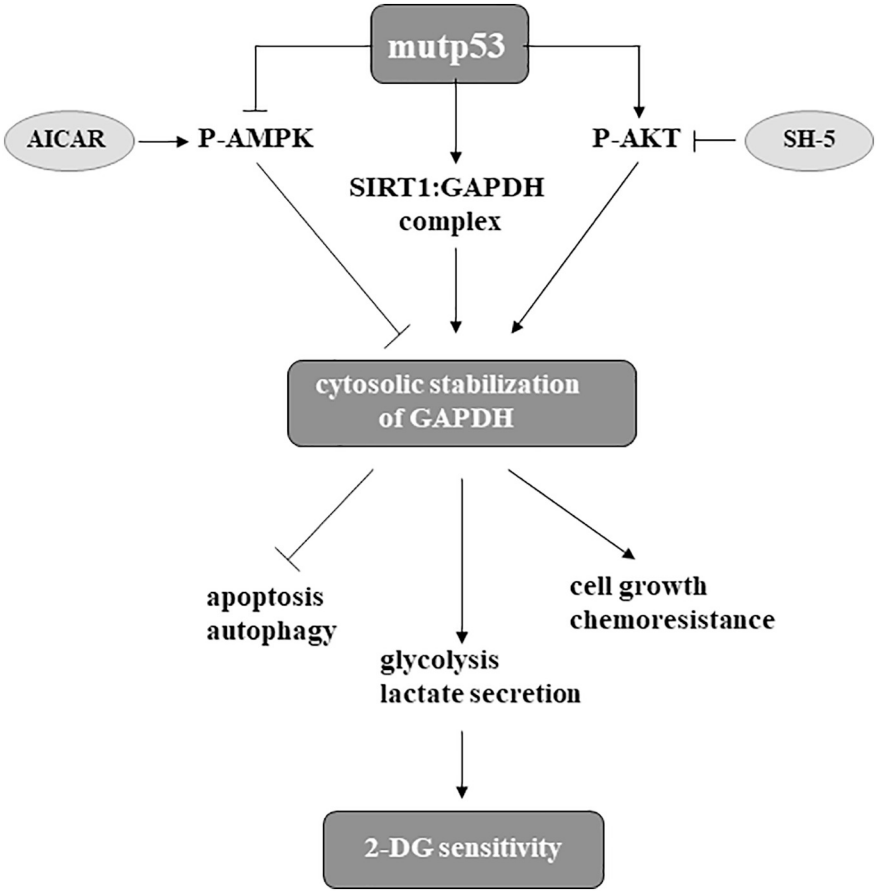

Fig. 6. Model of the insights identified in the present study.

and apoptosis after R273H mutp53 overexpression in AsPC1 cells with the concomitant inhibition of the cytosolic glycolytic activity of GAPDH by the AXP3009 compound or after GAPDH siRNA transfection for gene silencing. The effective capability of AXP3009 to inhibit GAPDH activity in PDAC cells and the silencing of GAPDH gene expression by siRNA were reported in Supplementary Fig. 1A and B, respectively. Fig. 4A and B show that a non-toxic concentration of AXP3009 or cell transfection with GAPDH siRNA reversed R273H mutp53-dependent PDAC cell hyperproliferation and apoptosis inhibition, respectively. To confirm the role of GAPDH cytosolic stabilization on the oncogenic effects of mutp53 we performed anchorage-independent soft agar colony assay. Fig. 4C shows that R273H mutp53 favors the formations of the colonies (as compared to mock cells) and that AXP3009 treatment strongly reversed this phenomenon in R273H cells. Similar results have been observed also for R175H mutp53-dependent modulation of cell growth and apoptosis (Supplementary Fig. 2A and B), extending the concept that GAPDH cytosolic stabilization may contribute to the oncogenic effects also of other GOF mutp53 isoforms.

Moreover, since we previously demonstrated that oncogenic effects of mutp53 in PDAC cells are mediated also by the counteraction of autophagy [28] and that mutp53s stimulate resistance to the drug gemcitabine in PDAC cells [31], we here investigated whether GAPDH activity might contribute to regulate also these phenomena. In Fig. 4D we demonstrated that mutp53 decreased the amount of intracellular autophagic vesicles and this event was completely reversed by the addition of the AMPK activator AICAr or the AKT inhibitor SH-5, which also restored GAPDH nuclear prevention by mutp53 (Fig. 3C) and reduced L-lactate secretion prompted by mutp53 (Fig. 3D). In accordance with these observations, the shp53-induced increase of autophagy was counteracted in GAPDH silencing conditions in Panc1 cells, confirming the involvement of GAPDH in the inhibition of autophagy by mutp53 (Fig. 4E). Altogether, these data indicate that GAPDH expression and its glycolytic activity are required to mediate several oncogenic effects of mutp53, including cancer cell hyper-proliferation, blockage of apoptosis and autophagy.

3.5. GAPDH cytosolic stabilization confers chemoresistance to gemcitabine and sensitizes cells to 2-deoxyglucose

Concerning drug chemoresistance, we demonstrated that GAPDH knock-down by siRNA restored PDAC cell sensitivity to gemcitabine even in mutp53-overexpressing conditions (Fig. 5A). Furthermore, we tested the role of GAPDH in PDAC cells endogenously expressing wild-type p53 or R273H mutp53. Fig. 5B shows that GAPDH silencing had an undetectable effect on gemcitabine sensitivity of WTp53 cells PaCa3 cells, while it enhanced the response to gemcitabine of mutp53 Panc1 cells.

Furthermore, we aimed to investigate whether PDAC cells bearing mutp53 might be more sensitive to the glycolytic standard inhibitor 2-DG, accordingly with the stimulatory role of mutp53 on glycolysis via GAPDH cytosolic stabilization. To functionally demonstrate the involvement of mutp53 on PDAC cell sensitivity to 2-DG, we evaluated the response of the cells after overexpression of R273H mutp53. Our data reported in Fig. 5C show that mutp53 overexpression conferred to p53-null AsPC1 cells a strong sensitization to 2-DG incubation, as compared to its negative mock control. These results demonstrated that targeting the glycolytic pathway may represent a potential therapeutic opportunity for cancer patients bearing mutations in the *TP53* gene.

4. Discussion

In addition to their canonical roles in glycolysis, recent studies uncovered some non-metabolic functions in tumorigenesis of glycolytic

enzymes, including GAPDH, providing important insights into the regulation of cancer cell growth and energetic metabolism [14]. Apart from glycolysis, GAPDH participates in apoptosis, autophagy, iron metabolism, membrane trafficking, histone biosynthesis, maintenance of DNA integrity and receptor mediated cell signaling. As such, GAPDH is not only a cytosolic protein but it can be detected in the membrane, the nucleus, polysomes, the ER and the Golgi of the cells [32]. GAPDH nuclear translocation is a particularly critical event in the light that, although the enzyme contains a nuclear export signal, it does not contain an equivalent nuclear localization signal. It has been demonstrated that a variety of post-translational modifications as well as protein-protein interactions are phenomena involved in the nuclear translocation of the enzyme [33], leading changes in gene expression profile and apoptosis in a number of cell systems [34,35]. Blocking this translocation was found to be sufficient to reduce cytotoxicity in cancer cells and to increase glycolytic activity, which is generally associated to cancer cell survival [17,36], thus GAPDH is also considered an attractive therapeutic target against cancer [37].

It is emerging that mutp53 proteins, contrarily to their wild-type p53 counterpart, stimulate glucose uptake and the Warburg effect of cancer cells, resulting in abnormal glycolytic pathway and cancer progression [38–40]. In the present study, we demonstrate that mutant p53 stimulates glycolysis and lactate secretion through the cytosolic stabilization of GAPDH, as schematically represented in Fig. 6. In particular, we show that mutant p53 can induce the expression of SIRT1, an evolutionary conserved deacetylase enzyme [41,42], which stimulates the proliferation and the expression of glycolytic genes in pancreatic neoplastic lesions [43]. In accordance with these observations, our data show that mutp53 stimulates lactate secretion with the concomitant upregulation of SIRT1 expression and the formation of SIRT1:GAPDH complex, which is reported to protect cytosolic GAPDH from nuclear translocation after various stimuli, retaining the glycolytic enzyme in the cytosol and promoting cell survival [21]. In line with this, Ventura et al. published that acetylation in various lysine residues of GAPDH is required for the nuclear translocation of the enzyme [44]. This would suggest that mutant p53 can protect cytosolic GAPDH from nuclear translocation through SIRT1-GAPDH binding and the consequent deacetylation of GAPDH. Furthermore, we reveal that another mechanism by which mutant p53 stabilizes GAPDH cytosolic localization is due to the stimulation of AKT and inhibition of AMPK signaling pathways, which are reported to directly phosphorylate GAPDH in different amino acidic residues with opposite effects on the nuclear translocation of the enzyme. Indeed, it has been previously demonstrated that AKT suppresses GAPDH-mediated apoptosis in ovarian cancer cells via phosphorylating GAPDH at Thr237 and decreasing its nuclear translocation [30], while AMPK stimulates the nuclear localization of GAPDH acting as a nuclear import signal [29]. We also demonstrate that the prevention of nuclear localization of GAPDH contributes to the oncogenic effects driven by mutant p53 in pancreatic cancer cells, as hyperproliferation, blockage of apoptosis and autophagy. Finally, a crucial evidence of the present manuscript is the demonstration that GAPDH is functionally involved in the mutp53-dependent chemoresistance to gemcitabine of PDAC cells. Therapeutically, the inhibition of GAPDH in order to restore PDAC cell sensitivity to gemcitabine may assume a critical relevance.

5. Conclusions

In conclusion, previous studies and the data of the present manuscript demonstrate that mutp53 isoforms contribute to enhance the glycolytic pathway in cancer cells through a coordinated regulation of both the expression and the subcellular localization of glycolytic enzymes, including the prevention of nuclear localization of GAPDH, thus favoring ATP production and the formation of metabolic intermediates for cancer cell growth. Intriguingly, from a therapeutic point of view, the stimulation of glycolysis by mutant p53 might represent an "Achilles heel" of cancer cells carrying mutant *TP53* gene, as revealed by the mutp53-dependent acquisition of cell sensitivity to the treatment with the glycolytic inhibitor 2-DG. Our results suggest that cancer cells expressing mutant p53 proteins can be significantly more sensitive to glycolytic drugs, as compared to the wild-type counterpart, providing new therapeutic opportunities to be further considered for clinical studies in cancer patients bearing mutant *TP53* gene.

Supplementary data to this article can be found online at https://doi.org/10.1016/j.bbamcr.2018.10.005.

Transparency document

The Transparency document associated with this article can be found, in online version.

Acknowledgments

This work was supported by Joint Projects program 2015 from University of Verona (Italy) to M. Donadelli (n. B12I15002320003).

Conflict of interest

The authors declare that they have no conflicts of interest.

References

[1] R. Siegel, J. Ma, Z. Zou, A. Jemal, Cancer statistics, 2014, CA Cancer J. Clin. 64 (1) (2014) 9–29.
[2] D.P. Ryan, T.S. Hong, N. Bardeesy, Pancreatic adenocarcinoma, N. Engl. J. Med. 371 (11) (2014) 1039–1049.
[3] D.D. Von Hoff, T. Ervin, F.P. Arena, E.G. Chiorean, J. Infante, M. Moore, et al., Increased survival in pancreatic cancer with nab-paclitaxel plus gemcitabine, N. Engl. J. Med. 369 (18) (2013) 1691–1703.
[4] J. Kleeff, M. Korc, M. Apte, C. La Vecchia, C.D. Johnson, A.V. Biankin, et al., Pancreatic cancer, Nat. Rev. Dis. Primers 2 (2016) 16022.
[5] M.P. Kim, G. Lozano, Mutant p53 partners in crime, Cell Death Differ. 25 (1) (2018) 161–168.
[6] M. Cordani, R. Pacchiana, G. Butera, G. D'Orazi, A. Scarpa, M. Donadelli, Mutant p53 proteins alter cancer cell secretome and tumour microenvironment: involvement in cancer invasion and metastasis, Cancer Lett. 376 (2) (2016) 303–309.
[7] J. Zhu, M.A. Sammons, G. Donahue, Z. Dou, M. Vedadi, M. Getlik, et al., Gain-of-function p53 mutants co-opt chromatin pathways to drive cancer growth, Nature 525 (7568) (2015) 206–211.
[8] M. Cordani, G. Butera, R. Pacchiana, M. Donadelli, Molecular interplay between mutant p53 proteins and autophagy in cancer cells, Biochim. Biophys. Acta 1867 (1) (2017) 19–28.
[9] S. Di Agostino, S. Strano, V. Emiliozzi, V. Zerbini, M. Mottolese, A. Sacchi, et al., Gain of function of mutant p53: the mutant p53/NF-Y protein complex reveals an aberrant transcriptional mechanism of cell cycle regulation, Cancer cell 10 (3) (2006) 191–202.
[10] P. Stambolsky, Y. Tabach, G. Fontemaggi, L. Weisz, R. Maor-Aloni, Z. Siegfried, et al., Modulation of the vitamin D3 response by cancer-associated mutant p53, Cancer cell 17 (3) (2010) 273–285.
[11] L. Weisz, A. Damalas, M. Liontos, P. Karakaidos, G. Fontemaggi, R. Maor-Aloni, et al., Mutant p53 enhances nuclear factor kappaB activation by tumor necrosis factor alpha in cancer cells, Cancer Res. 67 (6) (2007) 2396–2401.
[12] C. Zhang, J. Liu, Y. Liang, R. Wu, Y. Zhao, X. Hong, et al., Tumour-associated mutant p53 drives the Warburg effect, Nat. Commun. 4 (2013) 2935.
[13] F.M. Simabuco, M.G. Morale, I.C.B. Pavan, A.P. Morelli, F.R. Silva, R.E. Tamura, p53 and metabolism: from mechanism to therapeutics, Oncotarget 9 (34) (2018) 23780–23823.
[14] X. Yu, S. Li, Non-metabolic functions of glycolytic enzymes in tumorigenesis, Oncogene 36 (19) (2017) 2629–2636.
[15] L. Zheng, R.G. Roeder, Y. Luo, S phase activation of the histone H2B promoter by OCA-S, a coactivator complex that contains GAPDH as a key component, Cell 114 (2) (2003) 255–266.
[16] H. Nakajima, T. Kubo, H. Ihara, T. Hikida, T. Danjo, M. Nakatsuji, et al., Nuclear-translocated glyceraldehyde-3-phosphate dehydrogenase promotes poly(ADP-ribose) polymerase-1 activation during oxidative/nitrosative stress in stroke, J. Biol. Chem. 290 (23) (2015) 14493–14503.
[17] I. Dando, R. Pacchiana, E.D. Pozza, I. Cataldo, S. Bruno, P. Conti, et al., UCP2 inhibition induces ROS/Akt/mTOR axis: role of GAPDH nuclear translocation in genipin/everolimus anticancer synergism, Free Radic. Biol. Med. 113 (2017) 176–189.
[18] I. Dando, C. Fiorini, E.D. Pozza, C. Padroni, C. Costanzo, M. Palmieri, et al., UCP2 inhibition triggers ROS-dependent nuclear translocation of GAPDH and autophagic cell death in pancreatic adenocarcinoma cells, Biochim. Biophys. Acta 1833 (3) (2013) 672–679.

[19] I. Dando, M. Donadelli, C. Costanzo, E. Dalla Pozza, A. D'Alessandro, L. Zolla, et al., Cannabinoids inhibit energetic metabolism and induce AMPK-dependent autophagy in pancreatic cancer cells, Cell Death Dis. 4 (2013) e664.
[20] C.A. Tristan, A. Ramos, N. Shahani, F.E. Emiliani, H. Nakajima, C.C. Noeh, et al., Role of apoptosis signal-regulating kinase 1 (ASK1) as an activator of the GAPDH-Siah1 stress-signaling cascade, J. Biol. Chem. 290 (1) (2015) 56–64.
[21] H.Y. Joo, S.R. Woo, Y.N. Shen, M.Y. Yun, H.J. Shin, E.R. Park, et al., SIRT1 interacts with and protects glyceraldehyde-3-phosphate dehydrogenase (GAPDH) from nuclear translocation: implications for cell survival after irradiation, Biochem. Biophys. Res. Commun. 424 (4) (2012) 681–686.
[22] S. Ganapathy-Kanniappan, R. Kunjithapatham, J.F. Geschwind, Glyceraldehyde-3-phosphate dehydrogenase: a promising target for molecular therapy in hepatocellular carcinoma, Oncotarget 3 (9) (2012) 940–953.
[23] P.S. Moore, B. Sipos, S. Orlandini, C. Sorio, F.X. Real, N.R. Lemoine, et al., Genetic profile of 22 pancreatic carcinoma cell lines. Analysis of K-ras, p53, p16 and DPC4/Smad4, Virchows Arch. 439 (6) (2001) 798–802.
[24] S. Bruno, A. Pinto, G. Paredi, L. Tamborini, C. De Micheli, V. La Pietra, et al., Discovery of covalent inhibitors of glyceraldehyde-3-phosphate dehydrogenase, a target for the treatment of malaria, J. Med. Chem. 57 (17) (2014) 7465–7471.
[25] D.J. Klionsky, K. Abdelmohsen, A. Abe, M.J. Abedin, H. Abeliovich, A. Acevedo Arozena, et al., Guidelines for the use and interpretation of assays for monitoring autophagy (3rd edition), Autophagy 12 (1) (2016) 1–222.
[26] W. Ferdinand, The isolation and specific activity of rabbit-muscle glyceraldehyde phosphate dehydrogenase, Biochem. J. 92 (3) (1964) 578–585.
[27] A.S. Gomes, H. Ramos, J. Soares, L. Saraiva, p53 and glucose metabolism: an orchestra to be directed in cancer therapy, Pharmacol. Res. 131 (2018) 75–86.
[28] M. Cordani, E. Oppici, I. Dando, E. Butturini, E. Dalla Pozza, M. Nadal-Serrano, et al., Mutant p53 proteins counteract autophagic mechanism sensitizing cancer cells to mTOR inhibition, Mol. Oncol. 10 (7) (2016) 1008–1029.
[29] H.J. Kwon, J.H. Rhim, I.S. Jang, G.E. Kim, S.C. Park, E.J. Yeo, Activation of AMP-activated protein kinase stimulates the nuclear localization of glyceraldehyde 3-phosphate dehydrogenase in human diploid fibroblasts, Exp. Mol. Med. 42 (4) (2010) 254–269.
[30] Q. Huang, F. Lan, Z. Zheng, F. Xie, J. Han, L. Dong, et al., Akt2 kinase suppresses glyceraldehyde-3-phosphate dehydrogenase (GAPDH)-mediated apoptosis in ovarian cancer cells via phosphorylating GAPDH at threonine 237 and decreasing its nuclear translocation, J. Biol. Chem. 286 (49) (2011) 42211–42220.
[31] C. Fiorini, M. Cordani, C. Padroni, G. Blandino, S. Di Agostino, M. Donadelli, Mutant p53 stimulates chemoresistance of pancreatic adenocarcinoma cells to gemcitabine, Biochim. Biophys. Acta 1853 (1) (2015) 89–100.
[32] M.A. Sirover, Subcellular dynamics of multifunctional protein regulation: mechanisms of GAPDH intracellular translocation, J. Cell. Biochem. 113 (7) (2012) 2193–2200.
[33] M.A. Sirover, On the functional diversity of glyceraldehyde-3-phosphate dehydrogenase: biochemical mechanisms and regulatory control, Biochim. Biophys. Acta 1810 (8) (2011) 741–751.
[34] N. El Kadmiri, I. Slassi, B. El Moutawakil, S. Nadifi, A. Tadevosyan, A. Hachem, et al., Glyceraldehyde-3-phosphate dehydrogenase (GAPDH) and Alzheimer's disease, Pathol. Biol. 62 (6) (2014) 333–336.
[35] S. Hwang, M.H. Disatnik, D. Mochly-Rosen, Impaired GAPDH-induced mitophagy contributes to the pathology of Huntington's disease, EMBO Mol. Med. 7 (10) (2015) 1307–1326.
[36] C. Guo, S. Liu, M.Z. Sun, Novel insight into the role of GAPDH playing in tumor, Clin. Transl. Oncol. 15 (3) (2013) 167–172.
[37] G.S. Krasnov, A.A. Dmitriev, A.V. Snezhkina, A.V. Kudryavtseva, Deregulation of glycolysis in cancer: glyceraldehyde-3-phosphate dehydrogenase as a therapeutic target, Expert Opin. Ther. Targets 17 (6) (2013) 681–693.
[38] Y. Itahana, K. Itahana, Emerging roles of p53 family members in glucose metabolism, Int. J. Mol. Sci. 19 (3) (2018).
[39] H. Harami-Papp, L.S. Pongor, G. Munkacsy, G. Horvath, A.M. Nagy, A. Ambrus, et al., TP53 mutation hits energy metabolism and increases glycolysis in breast cancer, Oncotarget 7 (41) (2016) 67183–67195.
[40] I. Dando, M. Cordani, M. Donadelli, Mutant p53 and mTOR/PKM2 regulation in cancer cells, IUBMB Life 68 (9) (2016) 722–726.
[41] G.E. Simmons Jr., W.M. Pruitt, K. Pruitt, Diverse roles of SIRT1 in cancer biology and lipid metabolism, Int. J. Mol. Sci. 16 (1) (2015) 950–965.
[42] H.C. Chang, L. Guarente, SIRT1 and other sirtuins in metabolism, Trends Endocrinol. Metab. 25 (3) (2014) 138–145.
[43] A.V. Pinho, A. Mawson, A. Gill, M. Arshi, M. Warmerdam, M. Giry-Laterriere, et al., Sirtuin 1 stimulates the proliferation and the expression of glycolysis genes in pancreatic neoplastic lesions, Oncotarget 7 (46) (2016) 74768–74778.
[44] M. Ventura, F. Mateo, J. Serratosa, I. Salaet, S. Carujo, O. Bachs, et al., Nuclear translocation of glyceraldehyde-3-phosphate dehydrogenase is regulated by acetylation, Int. J. Biochem. Cell Biol. 42 (10) (2010) 1672–1680.